Heliyon 10 (2024) e29650

Contents lists available at ScienceDirect

Heliyon

journal homepage: www.cell.com/heliyon

Research article

A new gene signature associated with disulfidptosis that forecasts myasthenia gravis and suggests infiltration of immune microenvironment in thymoma patients

Yue Pan [a,b], Hongsheng Deng [a,b], Chao Yang [a], Lixuan Lin [a], Qi Cai [a], Jianxing He [a,*]

[a] *Department of Thoracic Surgery and Oncology, State Key Laboratory of Respiratory Disease, National Clinical Research Center for Respiratory Disease, Guangzhou Institute of Respiratory Health, the First Affiliated Hospital of Guangzhou Medical University, No.151, Yanjiang Road, 510120, Guangzhou, China*

[b] *Guangzhou Laboratory, No. 9 XingDaoHuanBei Road, Guangzhou International Bio Island, Guangzhou, 510005, Guangdong Province, China*

ARTICLE INFO

Keywords:
Thymoma-associated myasthenia gravis (TAMG)
Disulfidptosis
RNA-seq
Tumor immune microenvironment(TIME)

ABSTRACT

Introduction: The mechanism of thymoma-associated myasthenia gravis (TAMG) is currently unknown, although patients with TAMG experience more severe myasthenic symptoms and have worse prognoses compared to regular thymoma patients. The objective of this research is to create a transcriptome map of TAMG using genes linked to disulfidptosis, detect possible biomarkers, and examine the disparities in the tumor immune microenvironment (TIME) among different thymoma patients. The findings will offer valuable knowledge for personalized treatment alternatives.

Methods: Thymoma samples' RNA-seq data, along with their corresponding clinical data, were acquired from the TCGA database using methods. Next, genes and disulfidptosis-related lncRNAs (DRLs) were chosen through correlation analysis. Then, a prediction model of TAMG was established by LASSO regression. Subsequent to that, an analysis of the mutation data, the tumor mutational burden (TMB), and the assessment of immune and stromal elements within the tumor microenvironment were conducted.

Results: A total of 87 patients diagnosed with thymoma were included in the study, with 29 of them having TAMG. We discovered a group of 325 lncRNAs in this sample that showed significant associations with genes related to disulfidptosis, with 25 of them displaying significantly altered expression. Moreover, utilizing LASSO regression, we constructed a predictive model incorporating 11 DRLs. The analysis revealed an area under the curve (AUC) of 0.934 (CI 0.879–0.989), a cut-off value of 0.797, along with a sensitivity of 82.8 % and specificity of 93.1 %. Furthermore, we examined the TIME in both the high-risk and low-risk groups, and observed noteworthy disparities in B cells, T cells, and APC among the two groups ($p < 0.05$).

Conclusion: This research offers the initial examination of genes associated with disulfidptosis and TAMG through genomic and transcriptomic analysis. Furthermore, a strong risk forecasting model was created and the significance of TIME in TAMG was also clarified. The discoveries offer significant understanding into the molecular processes of TAMG and present possible indicators for categorizing risk.

* Corresponding author.
E-mail address: drjianxing.he@gmail.com (J. He).

https://doi.org/10.1016/j.heliyon.2024.e29650
Received 28 December 2023; Received in revised form 8 April 2024; Accepted 11 April 2024
Available online 15 April 2024

1. Introduction

Thymic epithelial tumors (TETs) are rare cancers found in the chest area, which present considerable difficulties in treatment because of their aggressive characteristics [1]. Cancer is caused by many changes within organisms and in the environment [2]. The DNA of the most vertebrates especially mammals is depleted in CpG dinucleotides [3]. The remaining CpGs clustering in DNA regions is generally referred to as CpG islands (CGIs). There has been growing interest in CGI because they are enriched in the promoters of genes [3] and by altering DNA methylation in CGIs, they play important roles in the regulation of gene expression and gene silencing in biological processes [4] and considerably, would help to discover the epigenetic causes of cancer [5].

Patients diagnosed with thymoma often experience autoimmune disorders, with around 33 % of cases showing these additional health conditions. Out of all the autoimmune conditions, myasthenia gravis (MG) stands as the prevailing one [6]. Individuals diagnosed with thymoma-associated myasthenia gravis (TAMG) experience heightened myasthenic symptoms and face bleaker prognoses [7]. While there are well-established diagnostic criteria for categorizing individuals with MG, a significant limitation exists due to the absence of objective biomarkers that can anticipate the advancement of the disease either in clinical settings or during clinical trials. Consequently, there is a pressing requirement for the creation of dependable biomarkers that can assist in the handling of these circumstances [8].

Currently, the precise understanding of TAMG remains uncertain, although scientists theorize that either the tumor cells or the atypical immune cells in the thymus gland might initiate an immune reaction against AChR or other elements of the neuromuscular junction [9–11]. The overexpression of specific genes has been linked to TAMG, and the reduced expression of CTLA-4 in thymoma could potentially heighten the vulnerability to developing MG [12,13].

Notably, the recently identified process of disulfidptosis differs from other well-known types of cell demise, as it is linked to the actin cytoskeleton, an essential component of cells that is vital for preserving cellular morphology and enhancing viability [14]. Moreover, it is believed that actin plays a role in the development of TAMG, which is linked to thymoma. Thymic selection, a crucial step in the maturation of immune cells, is thought to involve the actin cytoskeleton, a protein filament network that offers cells structure and support. Nevertheless, there is presently a lack of studies on TAMG-associated genes related to disulfidptosis.

Moreover, the epigenome comprising different mechanisms e.g. DNA methylation, remodeling, histone tail modifications, chromatin microRNAs and lncRNAs, interact with environ-mental factors like nutrition, pathogens, climate to influence the expression profile of genes and the emergence of specific phenotypes [4,15,16]. Multi-level interactions between the genome, epigenome and environmental factors might occur [17–19]. Furthermore, numerous lines of evidence suggest the influence of epigenome variation on health [3,20,21]. Also, the information obtained from the analysis of biological data by bioinformatics, in aligning sequences in information banks to find genetic similarities and differences, predicting the structure and function of gene products [22,23]. It helps to find the phylogenetic relationship between genes and protein sequences [24,25].

Hence, the objective of this research was firstly to chart the transcriptome of TAMG using genes linked to disulfidptosis. Our goal was to detect potential biomarkers for the diagnosis and treatment of TAMG by screening risk genes and developing a prediction model. Furthermore, we examined the disparities in tumor immune microenvironment (TIME) among TAMG patients classified as high and low-risk groups, aiming to offer recommendations for personalized treatment choices. The findings of this research could greatly enhance our comprehension of the molecular processes that underlie TAMG and contribute to the creation of improved and tailored therapeutic approaches for this critical ailment.

2. Materials and methods

2.1. Raw data

Data from the TCGA database (https//portal.gdc.cancer.gov/) included 94 thymoma patients with clinical data and corresponding transcriptome RNA-seq data of 92 samples (2 normal cases and 90 tumor cases). Additionally, mutome data of the patients were also obtained. Out of the 90 tumor samples in the transcriptome data, 3 cases did not have information on MG. Supplementary Table 1 showed the detailed raw data. Gene IDs from the Human Genome Annotated Data (GRCh38) were used to annotate the clinical data of the patients. The annotations were carried out utilizing the online resource found at https://asia.ensembl.org/index.html. The research follows the data access protocols and publication standards set by TCGA.

2.2. Development of a genetic marker linked to myasthenia gravis and disulfidptosis

Genes associated with disulfidptosis were obtained from the available literature [14]. In particular, disulfidptosis-related lncRNAs (DRLs) were chosen using correlation analysis (with a corFilter of 0.4 and pvalueFilter of 0.001). The variable selection and shrinkage process was performed using the 'glmnet' R package, utilizing the Least Absolute Shrinkage and Selection Operator (LASSO) algorithm. In the TCGA cohort, the status of patients' TAMG was determined by the DRLs, which served as the independent variable. Tenfold cross-validation was used to determine the penalty parameter (λ) for the model, based on the minimum criteria. This criteria corresponds to the value of λ that yields the lowest partial likelihood deviance. The risk scores of patients were determined by evaluating the expression level of every gene and their respective regression coefficients, following the formula score = sum (expression of each gene $\times$ corresponding coefficient) [26]. Subsequently, the predictive capability of the genetic pattern was assessed through analysis of the ROC curve. Ultimately, the individuals were categorized into high-risk and low-risk categories by utilizing the median value of the risk

score [26]. Subsequently, principal component analysis (PCA) was performed using the 'prcomp' function from the 'stats' R package, considering the gene expression in the signature [27].

2.3. Gene set enrichment

The 'clusterProfiler' R package was utilized to conduct analysis on the differentially expressed genes (DEGs) with a fold change of $|\log2FC| \geq 1$ and a false discovery rate (FDR) of <0.05 between the high-risk and low-risk groups, using Gene Ontology (GO) and Kyoto Encyclopedia of Genes and Genomes (KEGG) methods. The target sets for Gene Set Enrichment Analysis (GSEA) were downloaded from the Molecular Signatures Database as Analysis Hallmark and c2.cp.kegg.v7.2.symbols.gmt. GSEA-3.0 software from Broad Institute was used to perform the analysis.

2.4. Mutation landscape

We utilized the R package maftools [28] to analyze the mutation data, enabling us to assess the enrichment of oncogenic pathways in primary tumors from TCGA. TMB, which stands for tumor mutational burden, was determined by analyzing SNV data from primary tumors. TMB represents the overall count of somatic mutations found in a tumor sample per megabase (Mb).

2.5. Generation of ImmuneScore, StromalScore, and ESTIMATEScore

For each sample, the immune-stromal component ratio in the tumor microenvironment (TME) was calculated using the ESTIMATE algorithm, which was implemented in R version 4.0.2 and utilized the estimate package. The algorithm produced three scores: ImmuneScore, StromalScore, and ESTIMATEScore, which represented the proportion of immune, stromal, and the combined sum of both elements, respectively [29]. A greater percentage of the corresponding component in the TME was indicated by higher scores. Following the analysis, the CIBERSORT computational technique was utilized to estimate the abundance profile of tumor-infiltrating immune cells (TIC) in every tumor sample [30].

2.6. Statistical analysis

Before conducting the analysis, numerical and percentage representations were used to describe categorical variables, while means and standard deviations were employed to express measurement data that followed a normal distribution. Data that did not follow a

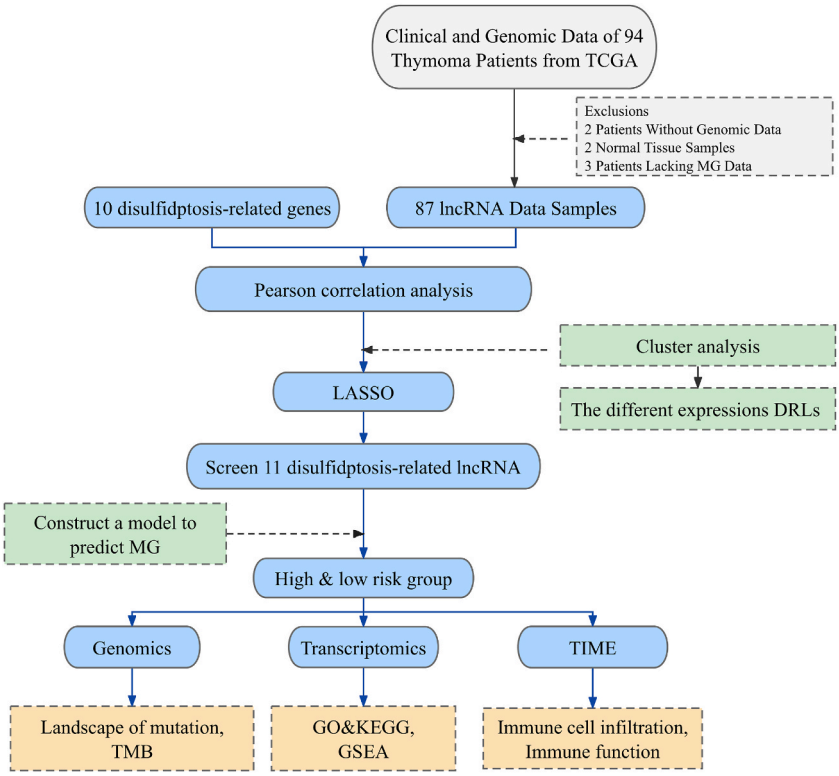

Fig. 1. The workflow chart of this study. DRLs, disulfidptosis-related lncRNAs.

normal distribution were described by calculating the medians and interquartile range (IQR). To compare the variations in proportions between groups, we conducted Pearson's χ2 test, Fisher's exact test, and nonparametric tests. Additionally, we calculated correlations using Pearson correlation analysis and Spearman rank correlation analysis. The statistical analysis was conducted utilizing R software (version 4.2.2). In conclusion, any test with a p value below 0.05 was deemed to have statistically significant results, and all p values mentioned in the document are two-tailed unless specified otherwise.

3. Results

3.1. 1Clinical characteristics

Fig. 1 displays the depicted workflow diagram for this study. A total of 87 patients diagnosed with thymoma were included in our study, with 29 of them having MG. The individuals diagnosed with MG had a median age of 55 years (ranging from 17 to 79 years), comprising of 14 male and 15 female patients. On the other hand, those without MG had a median age of 61 years (ranging from 39 to 81 years), consisting of 30 male and 28 female patients. Six distinct categories were assigned to the thymic tumors, including A type (n

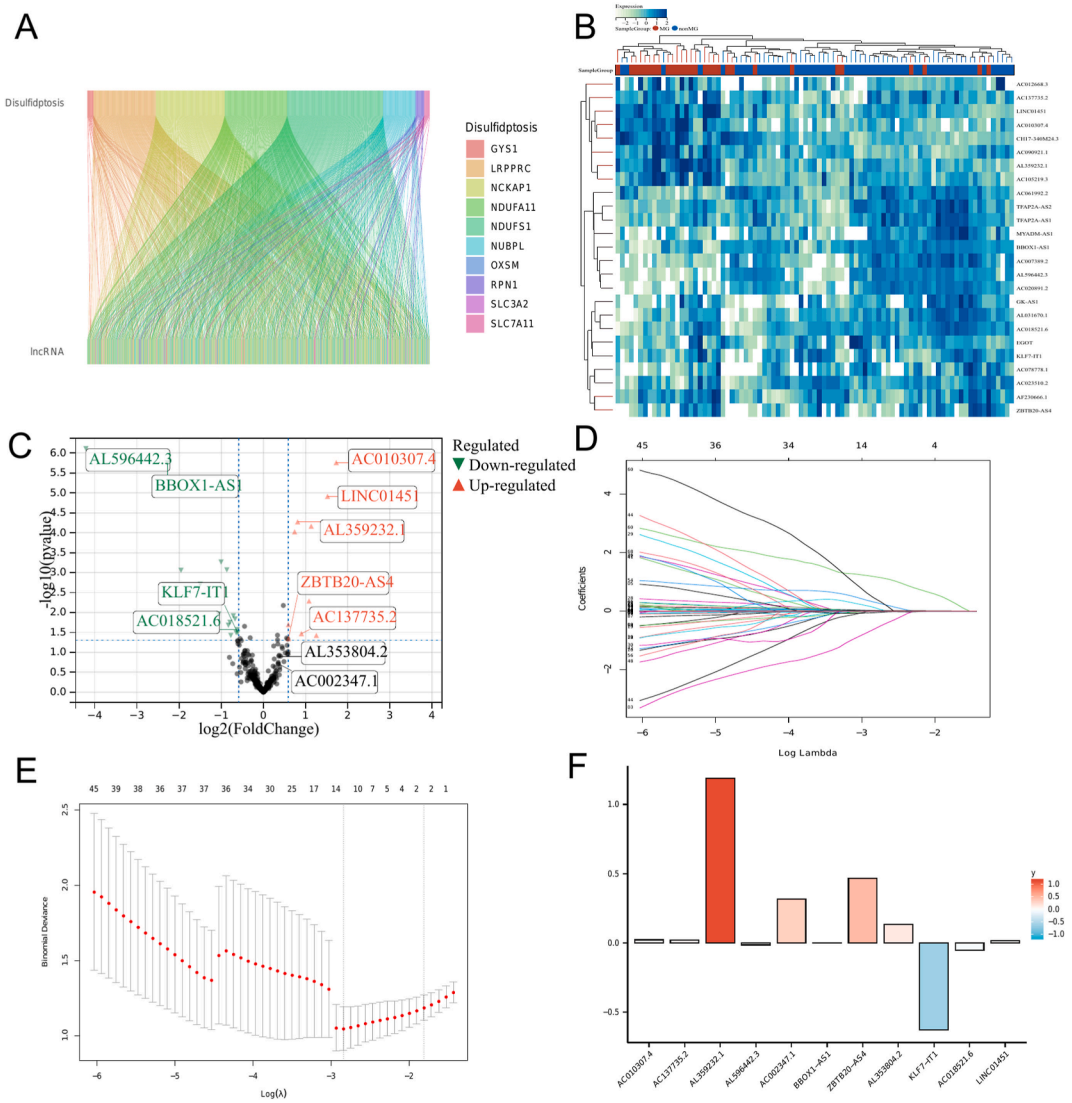

Fig. 2. Identification of the DRLs signature using LASSO regression. (A) The co-expression analysis of disulfidptosis-related genes and lncRNAs. (B) Heatmap analysis of DRLs in patients with thymoma with MG and patients without MG. (C) Differential expression of DRLs between thymoma with MG and thymoma without MG. (D) The log (lambda) sequence plot of DRLs using LASSO regression. (E) The LASSO coefficient profiles of DRLs. (F) DRLs and coefficients selected by LASSO regression. DRLs, disulfidptosis-related lncRNAs; LASSO, Least Absolute Shrinkage and Selection Operator; MG, myasthenia gravis.

= 11), AB type (n = 26), B1 type (n = 10), B2 type (n = 22), B3 type (n = 9), and thymic carcinoma (TC) (n = 9) (Supplementary Table 2). No significant disparities in age, gender, or Masaoka stage were found when comparing patient characteristics in the two groups. Nevertheless, we noticed a notable disparity in the allocation of WHO categorization [31] ($p < 0.01$) (Supplementary Table 2).

3.2. Disulfidptosis-related gene expression in TAMG

Through the examination of gene co-expression, we discovered a collection of 325 lncRNAs that displayed a strong correlation with genes related to disulfidptosis (Fig. 2A). In thymoma patients, we examined the expression of these DRLs in both MG+ and MG-groups. We discovered 25 DRLs that exhibited significant differences in expression, with 10 showing up-regulated expression and 15 showing down-regulated expression (Fig. 2B-C, Supplementary Table 3).

In order to further investigate the possibility of inferring TAMG status using gene expression profiles, we additionally utilized a LASSO regression model (Fig. 2D–E). The findings showed that a model consisting of 11 genes (AC010307.4, AC137735.2, AC137735.2, AL596442.3, AL596442.3, AL596442.3, ZBTB20-AS4, AL353804.2, AL353804.2, AL353804.2, and AL353804.2) demonstrated the highest accuracy in predicting outcomes (Fig. 2F). Further investigation was conducted on the SLC7A11, SLC3A2, RPN1, NCKAP1, NUBPL, NDUFA11, LRPPRC, OXSM, NDUFS1, and GYS1 mRNAs, as well as the co-expressed DRLs that were identified. The correlation analysis indicated that AL359232.1 exhibited a positive correlation with NUBPL ($r = 0.506$, $p < 0.001$), GYS1 ($r = 0.408$, $p < 0.001$), and OXSM ($r = 0.364$, $p < 0.01$), while demonstrating a negative correlation with RPN1 ($r = -0.345$, $p < 0.001$). Furthermore, NDUFS1 showed a positive correlation with ZBTB20−AS4 ($r = 0.557$, $p < 0.001$), AC018521.6 ($r = 0.769$, $p < 0.001$),

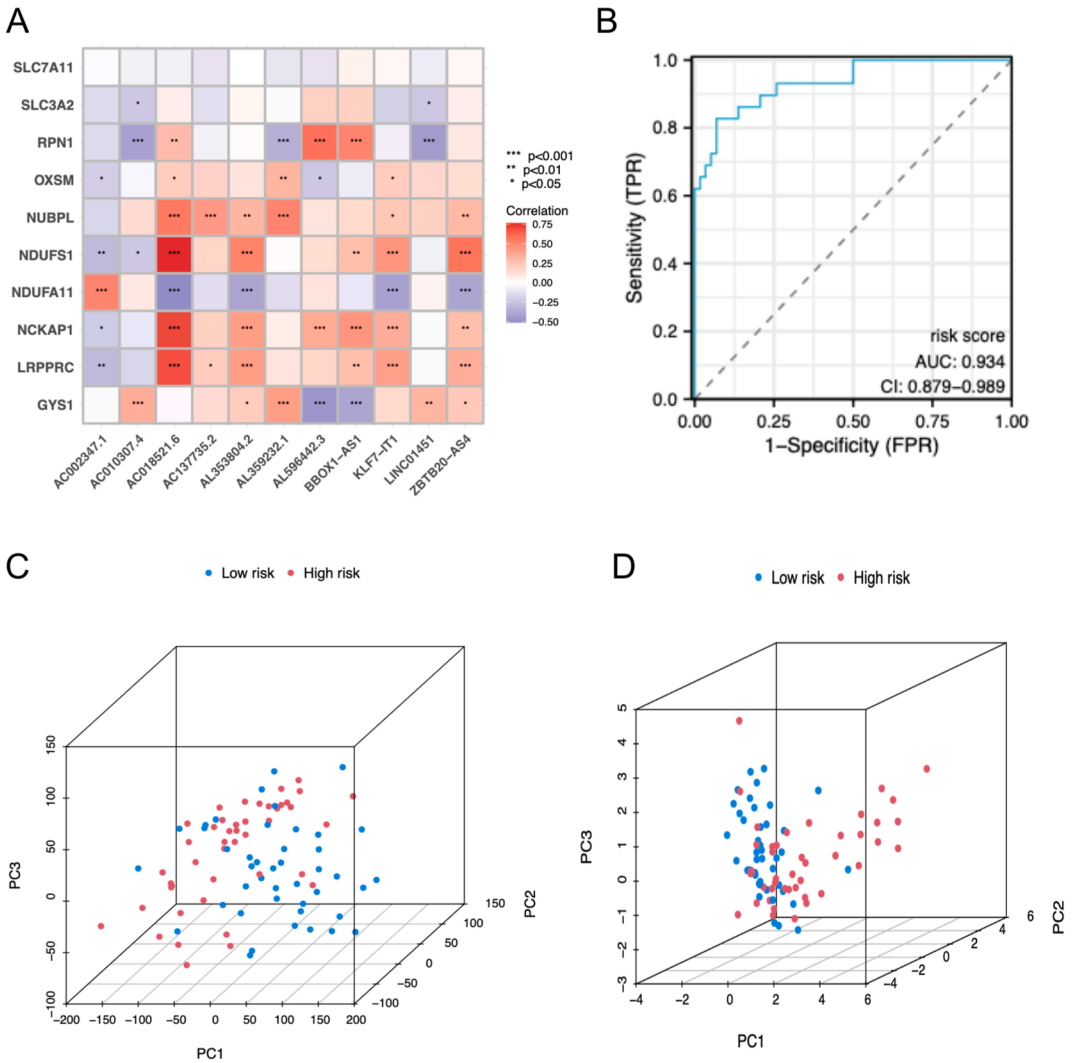

Fig. 3. A predictive model incorporating 11 DRLs for predicting TAMG. (A)ROC curves verified the TAMG of the risk score. (B) Association of the 11 DRLs included in the prediction TAMG model with disulfidptosis-related genes. DRLs, disulfidptosis-related lncRNAs; TAMG, thymoma-associated myasthenia gravismyasthenia gravis; ROC, receiver operator characteristic curve.*$p < 0.05$, **$p < 0.01$, ***$p < 0.001$.

NCKAP1 (r = 0.705, p < 0.001), LRPPRC (r = 0.690, p < 0.001), and NUBPL (r = 0.570, p < 0.001), while exhibiting a negative correlation with NDUFA11 (r = −0.506, p < 0.001) (Fig. 3A).

In Fig. 3B, the AUC for predicting TAMG was 0.934 (CI 0.879–0.989), with a cut-off of 0.797, demonstrating a sensitivity of 82.8 % and specificity of 93.1 %. After calculating the median risk score as 0.347, we categorized thymoma patients into low- and high-risk groups depending on whether their risk score was below or above the median. PCA was subsequently conducted to assess the capacity of the chosen genes in discriminating high- and low-risk TAMG groups from the entire gene set. The outcomes demonstrated that the chosen genes were capable of effectively distinguishing between the two groups, thereby confirming the reliability of our risk score model (Fig. 3C–D).

3.3. Functional and pathway enrichment analysis of genes with differential expression

Following the completion of GO functional enrichment analysis, it was discovered that the genes associated with differential risk were notably enriched in functions pertaining to the extracellular matrix containing collagen, organization of external encapsulating structures, and the structural constituent of the extracellular matrix (Fig. 4A). Furthermore, the KEGG pathway enrichment analysis revealed a significant enrichment of these genes in the ECM receptor interaction pathway, focal adhesion pathway, and the PI3K−Akt signaling pathway (Fig. 4B). In addition, GSEA analysis showed that the high-risk group had significant enrichment of pathways related to oxidative phosphorylation, ribosomes, and systemic lupus erythematosus. On the other hand, the low-risk group had significant enrichment of pathways such as ECM receptor interaction, focal adhesion, pathways in cancer, and the TGF beta signaling pathway (Fig. 4C–D).

3.4. The mutational landscape of TETs

Missense mutation was the most frequent variant classification in both the high-risk and low-risk groups, while SNP was the most prevalent variant type. Fig. 5A shows the high-risk group's top 10 mutation genes as GTF2I, TTN, RAB3GAP2, NEXMIF, MYO15A,

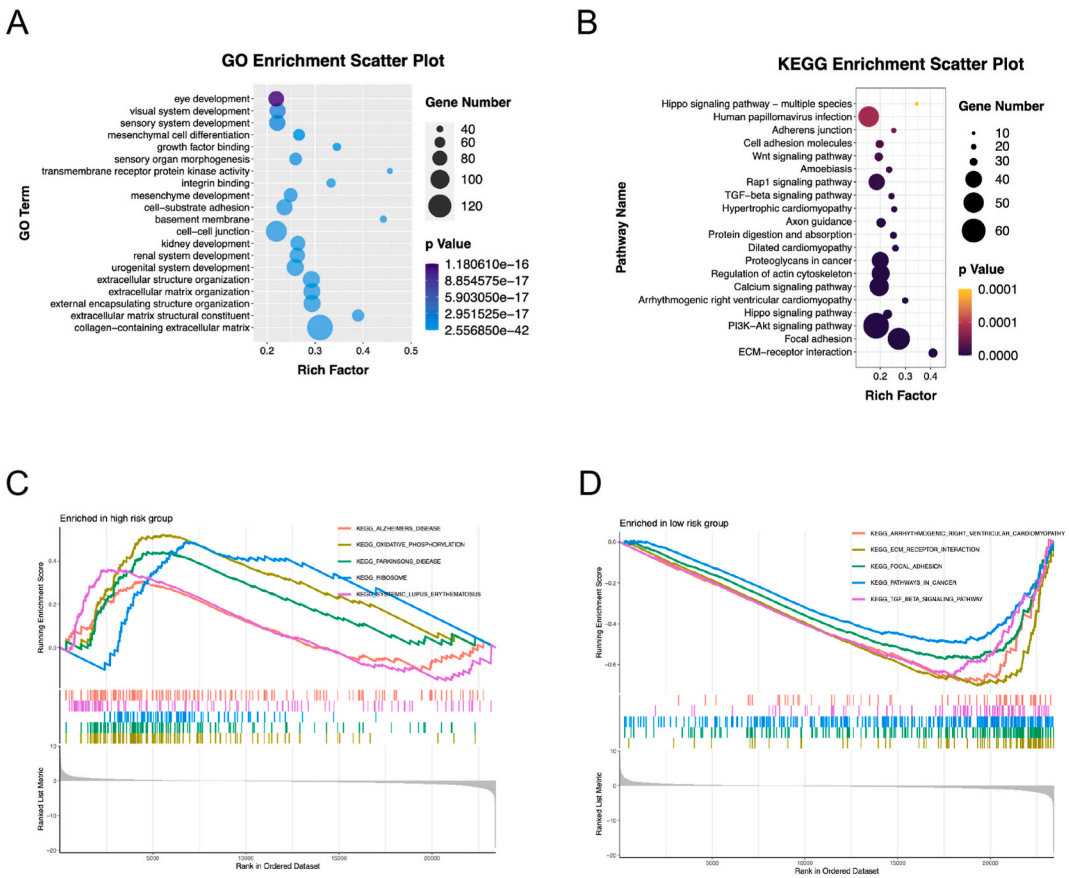

Fig. 4. Functional and pathway enrichment analysis of differentially expressed DRLs. (A)Bubble graph of GO enrichment analysis of differentially expressed DRLs. (B) KEGG analysis of differentially expressed DRLs. (C)GSEA analyses of differentially expressed DRLs in high-risk group. (D)GSEA analyses of differentially expressed DRLs in low-risk group. DRLs, disulfidptosis-related lncRNAs; GO, Gene Ontology; KEGG, Kyoto Encyclopedia of Genes and Genomes; GSEA, Gene Set Enrichment Analysis.

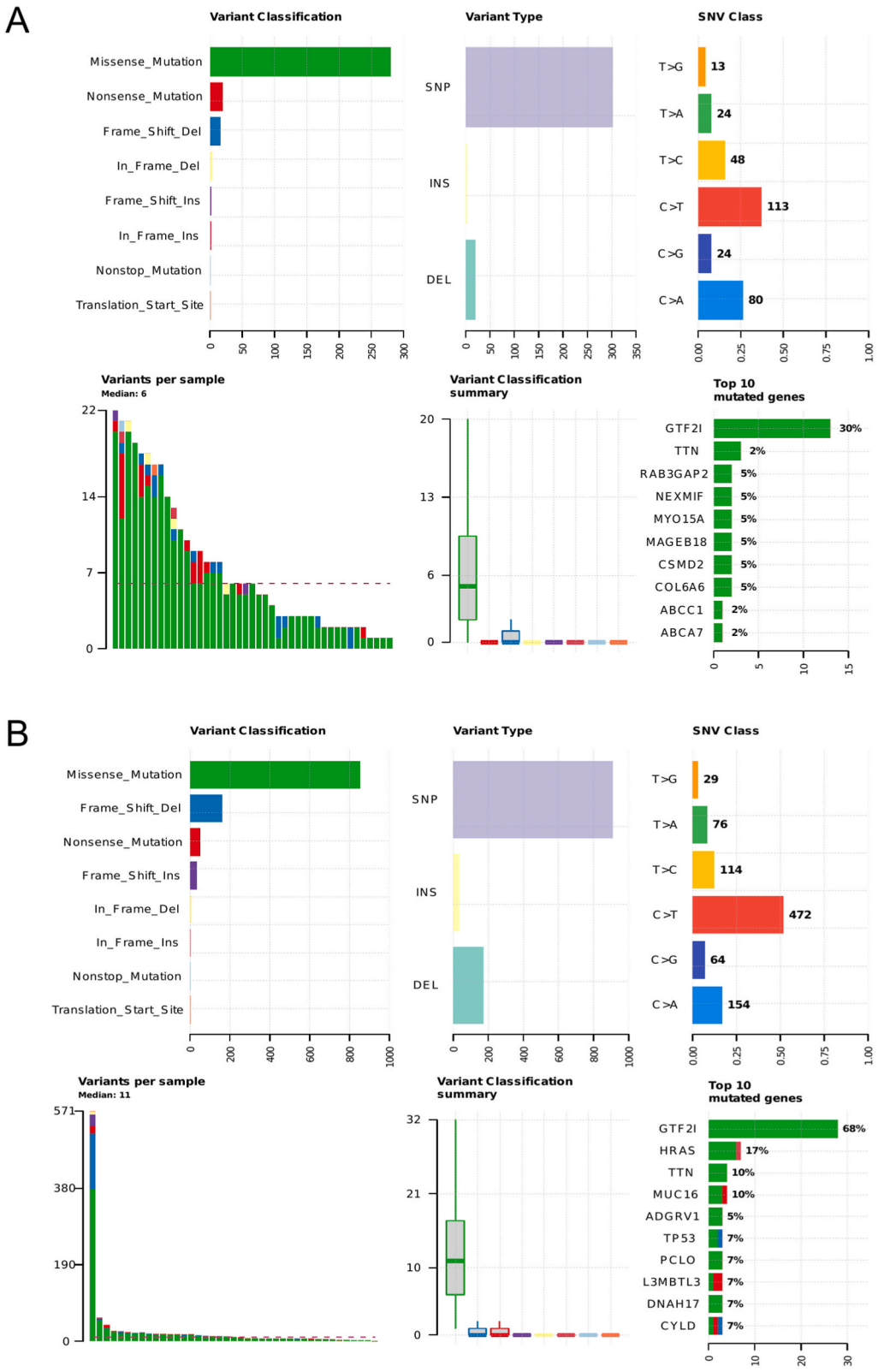

Fig. 5. The Mutational Landscape of TETs. (A)The mutation information of genes with high mutation frequency in high-risk group. (B)The mutation information of genes with high mutation frequency in low-risk group. TETs, thymic epithelial tumor.

MAGEB18, CSMD2, COL6A6, ABCC1, and ABCA7. The low-risk group had the following top 10 mutation genes: GTF2I, HRAS, TTN, MUC16, ADGRV1, TP53, PCLO, L3MBTL3, DNAH17, and CYLD (Fig. 5B). Moreover, the TMB of the low-risk cohort exceeded that of the high-risk cohort (0.368 compared to 0.249, $p = 0.00062$) (Supplementary Fig. 1).

3.5. The immune microenvironment of the high- and low-risk categories

The high-risk group, analyzed with the ESTIMATE algorithm, exhibited elevated ImmuneScore (2212 vs. 1,826, $p < 0.01$) and decreased StromalScore (−246.2 vs. −567.2, $p < 0.01$) in comparison to the low-risk group (Fig. 6A). In the high- and low-risk groups, Fig. 6B displays the proportions of different types of immune cells including B cells, T cells, natural killer cells, macrophages, dendritic cells (DC), and their subcategories.The group at high risk exhibited a higher number of plasma cells, an increased presence of T cell follicular helper (Tfh), and a greater activation of DC compared to the low-risk group (all $p < 0.05$). Nevertheless, there was no notable disparity in $CD8^+$ T lymphocytes or T regulatory cells among the two cohorts (Fig. 6C). Furthermore, the variances in immune function scores between the high and low risk groups were primarily focused on APC co-inhibition, B cells, checkpoint, cytolytic activity, DCs, HLA, mast cells, T cell co-inhibition, T cell co-stimulation, Tfh, Th1, and TIL.In all of these aspects, the high-risk group outperformed the low-risk group (Fig. 6D).

4. Discussion

For the first time, a thorough examination of genes associated with disulfidptosis was conducted in this study to investigate TAMG, yielding noteworthy findings that establish a notable connection between disulfidptosis-related genes and TAMG. Furthermore, an exceptional risk prediction model was developed with outstanding predictive capabilities. Using our risk prediction model, we examined the TIME in high- and low-risk categories and observed noteworthy variances in B cells, T cells, and APC between these two groups. The results indicate that the genes linked to increased risk in MG might engage with immune cells, resulting in the disruption of muscle actin and ultimately contributing to the emergence of TAMG.

Currently, there is still a lack of complete comprehension regarding the pathological and physiological mechanisms that underpin

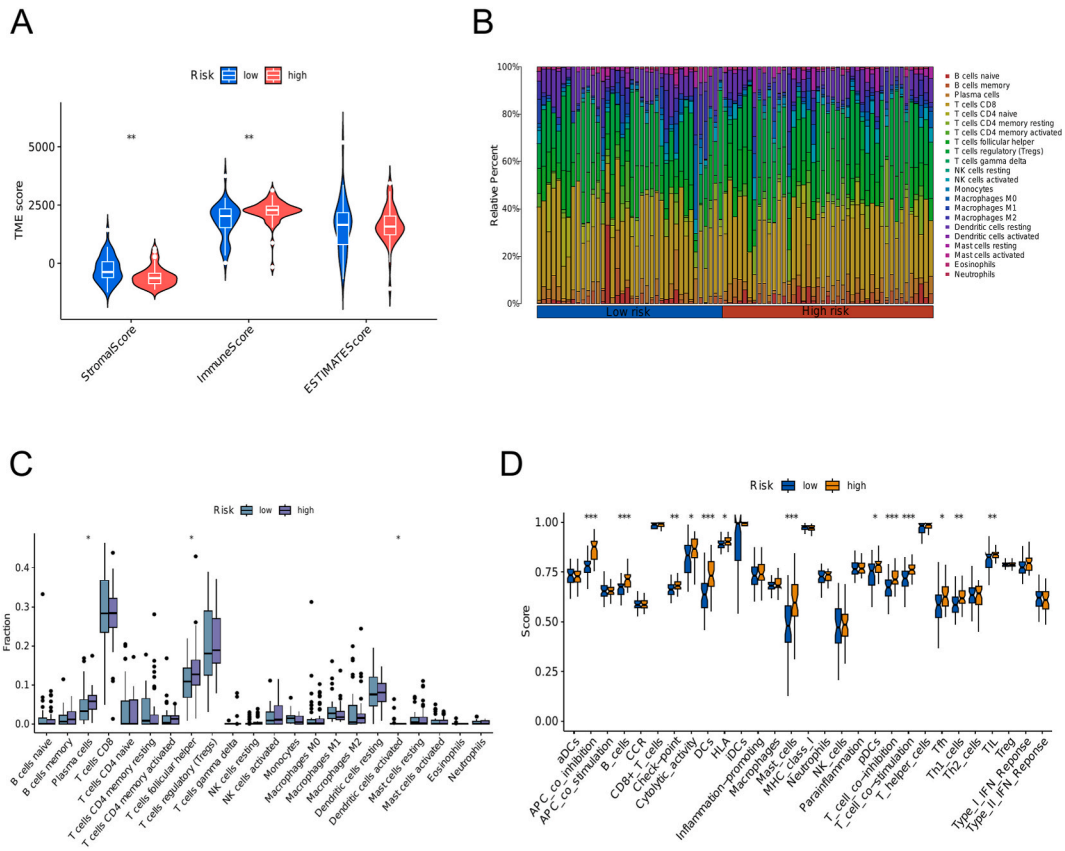

Fig. 6. The Immune Microenvironment of the High and Low Risk Groups. (A)ESTIMATE algorithm in high- and low-risk groups. (B)The percentages of various immune cells in high- and low-risk groups. (C)The immune cell infiltration in high- and low-risk groups. (D)The immune function scores in high- and low-risk groups. *$p < 0.05$, **$p < 0.01$, ***$p < 0.001$.

TAMG. Further research is needed to explore the specific mechanisms behind thymoma, as numerous studies have indicated its association with immune system abnormalities and their impact on the immune system's recognition of self-antigens [10,32]. Furthermore, TAMG could potentially be linked to other elements like irregularities in neurotransmitters and harm to the neuromuscular junction. Hence, additional investigation is required to acquire a more profound comprehension of the etiology and therapeutic approaches for this ailment. With the advancement of gene sequencing technology in recent years, it is possible that specific transcriptome genes play a role in the progression of TAMG. An instance of thymoma exhibits high levels of expression of a gene for mid-sized neurofilament, which contains similar genetic codes for acetylcholine receptors and titin epitopes, and is frequently associated with MG [12]. For example, NEFM displays restricted sequence resemblance to primary autoimmune targets, while RYR3 demonstrates significant similarity [12]. Furthermore, prior research has shown that alterations in the expression of lncRNAs can play a crucial role in differentiating TAMG and uncovering the molecular mechanisms that contribute to its development [33,34]. Nevertheless, there has been no inquiry into the possible participation of DRLs. Hence, considering the proof provided in this document, it seems that the expression of genes associated with disulfidptosis can control multiple signaling pathways that play a role in the formation of TAMG.

Initially, we employed correlation analysis to identify genes associated with disulfidptosis. Furthermore, LASSO regression (Fig. 2F) enabled the identification of 11 genes associated with TAMG. The involvement of these genes encompasses a range of cellular processes, including cellular transportation and the synthesis of proteins. Crucially, all 11 genes were discovered to have a connection with disulfidptosis. Moreover, the well-established risk assessment model demonstrated excellent diagnostic effectiveness for TAMG, suggesting a strong correlation between TAMG and disulfidptosis in tumors. Nevertheless, there have been no reports linking TAMG with disulfidptosis-related genes like SLC7A11, SLC3A2, and GYS1. Apoptosis in animal experiments previously entailed caspase-mediated gelsolin cleavage, resulting in heightened actin filament fragmentation and cleavage of the myosin-activating kinase ROCK. As a consequence, myosin-induced contractile activity was hyperactivated, leading to the generation of blebs in the process of apoptosis [35]. Identifying a novel mechanism underlying disulfidptosis, characterized by the collapse of the cytoskeleton initiated by disulfide bond formation, opens up exciting avenues for exploring potential targets to modulate this specific type of cell death [36]. TAMG may occur due to the overexpression of the mentioned risk genes, which can potentially cause malfunctioning of myosin and disruption of the cellular skeleton, ultimately resulting in the progression of TAMG.

The TETs in TIME is composed of various groups of innate and adaptive immune cells with different characteristics that display a varied distribution throughout the tumor [37]. Thymic cancers are linked to disturbed structure of the thymus and decreased or missing presence of MHC class II and AIRE factor. The outcome of this is expected to lead to the unsuccessful process of selecting both positive and negative thymocytes or a decrease in the generation of regulatory T cells [10]. In this research, we discovered that there were variations in both the quantity and performance of B lymphocytes among the high- and low-risk categories. Recent studies have focused on exploring and understanding the role of B cells in tumor immunity and their connection to the presence of thymic germinal centers (GCs) in the neighboring tissues of thymomas. These thymomas are enclosed by high endothelial venules (HEVs), which are recognized for their ability to attract peripheral cells. Furthermore, individuals with TAMG exhibit elevated concentrations of IFN-γ, IL-1β, and sCD40L in their serum [38].

The reduction in thymic macrophages hinders the removal of dying thymocytes and promotes the liberation of internal genetic material from dead thymic cells. In this inflammatory state, thymic epithelial cells have the potential to excessively produce IFN-β, which specifically triggers α-AChR expression, causing self-sensitization and thymic changes that ultimately lead to AChR-MG. The results emphasize the intricacy of the immune system [39]. In our study, we observed variations in B cells between the high- and low-risk groups of TAMG. However, it is worth noting that the disparity in IFN did not reach statistical significance. The complexity of thymoma's TIME and the variety of factors contributing to TAMG are implied by this.

Besides B cells, which are the main contributors to the production of autoantibodies, T lymphocyte subsets, particularly T helper cells, also have a vital function in TAMG. T helper cells have the ability to start and maintain long-lasting inflammation, enhance inflammatory signals, influence class switching and somatic hypermutation, and transform B cells into plasma cells that generate autoantibodies [11]. Ultimately, these processes result in the growth and advancement of MG.

Due to the absence of any immunological signature or lymphocyte activation in TAMG, it seems more likely that the prevailing mechanism underlying targeted anti-muscle autoimmunity in TAMG is "false-positive selection" driven by MHC-bound autoantigen-derived peptides [12], though there may be other underlying mechanisms. The immune dysfunctions witnessed in individuals with thymoma are probably a result of a blend of mechanisms. Additional research is required to clarify the fundamental processes accountable for immune dysfunction in individuals with thymoma.

The removal of the thymus gland can be considered as a successful treatment in changing the development from ocular myasthenia gravis to generalized myasthenia gravis [40]. TETs exhibit high expression of PD-1 and PD-L1, two vital immune checkpoints, which can potentially indicate the progression of TETs and the effectiveness of immunotherapy. Nonetheless, the use of ICIs in TETs is associated with a notably elevated occurrence of immune-related adverse events (irAEs) in contrast to other forms of cancer [41]. Despite the ongoing research on various immunotherapies for TETs, most of them are still in the experimental or preclinical phases.

In recent times, there has been a shift in cancer treatment towards therapies that target molecules. Nevertheless, the rarity and histological heterogeneity of TET pose a challenge to new treatment development [42]. Individuals identified with TETs, irrespective of their particular histopathology, additionally exhibit an inexplicable tendency towards the emergence of autoimmune toxicity impacting the muscular or neuromuscular system [43]. Hence, these DRLs have the potential to function as indicators for distinguishing thymoma with or without MG. Moreover, these molecules associated with the development of diseases may hold promise as targets for treatment.

While this study has produced significant findings, it is crucial to acknowledge the various constraints that should be taken into

account. Further research is needed to validate the precise molecular functions of the identified DRLs, as the initial sample size was relatively small, thus requiring additional support for our findings. Furthermore, the dataset employed did not contain data on AChR, which is recognized to have a connection with TAMG. Hence, it is necessary to conduct further investigations to examine the possible correlation between the lncRNAs analyzed in the study and AChR. This exploration could offer valuable additional knowledge regarding the fundamental mechanisms of TAMG.

A limitation of this study is the reliance on retrospective data sources. Future research could benefit from the inclusion of prospective data. Additionally, while our findings are promising, the sample size could be expanded further. Incorporating a multi-center patient cohort would not only enhance the generalizability of our results but also provide a more robust validation of the identified lncRNAs as potential biomarkers for TAMG. Moreover, future studies could employ single-cell sequencing technologies to offer a more detailed interpretation of immune cell infiltration within the TIME.

5. Conclusion

By conducting bioinformatic analysis on thymoma patients from the TCGA dataset, we discovered a group of genes related to disulfidptosis that were linked to TAMG. Among these, 11 DRLs stood out for their association with TAMG, specifically AL359232.1, ZBTB20-AS4, AC002347.1, KLF7-IT1, among others. Utilizing this information, we created a risk prediction model for TAMG. Functional pathways associated with the immune and nervous systems may be involved in regulating the development of TAMG through the target genes of the identified lncRNAs. The high-risk genes may interact with immune cells, causing dysregulation of muscle actin and leading to the development of TAMG. The results indicate a notable progress in the TAMG field and establish a basis for future studies on the molecular mechanisms involved in disulfidptosis and its impact on cellular balance.

Ethics declarations

Review and/or approval by an ethics committee was not needed for this study because the information was obtained from the TCGA repository, and it was utilized in a morally sound manner.

Agreement to make information public

Does not apply.

Data availability statement

Data from TCGA database (https://portal.gdc.cancer.gov/) including transcriptome RNA-seq data and relevant clinical data were obtained. The analyzed datasets generated during the study are available from the corresponding author upon reasonable request.

Funding

The writers affirm that they did not receive any financial assistance, grants, or other forms of support while preparing this manuscript.

CRediT authorship contribution statement

Yue Pan: Formal analysis, Data curation, Conceptualization. **Hongsheng Deng:** Validation, Supervision. **Chao Yang:** Validation, Software. **Lixuan Lin:** Software, Methodology. **Qi Cai:** Supervision, Software. **Jianxing He:** Writing – review & editing.

Declaration of competing interest

The authors declare that they have no known competing financial interests or personal relationships that could have appeared to influence the work reported in this paper.

Acknowledgements

The writers express their gratitude to AiMi Academic Services (www.aimieditor.com) for providing English language editing and reviewing assistance.

Appendix A. Supplementary data

Supplementary data to this article can be found online at https://doi.org/10.1016/j.heliyon.2024.e29650.

References

[1] C. Basse, N. Girard, Thymic tumours and their special features, Eur. Respir. Rev. 30 (162) (2021).
[2] M.R. Mohammadabadi, M.R. Mozafari, Enhanced efficacy and bioavailability of thymoquinone using nanoliposomal dosage form, J. Drug Deliv. Sci. Technol. 47 (2018) 445–453.
[3] A. Barazandeh, et al., Genome-wide analysis of CpG islands in some livestock genomes and their relationship with genomic features, Czech J. Anim. Sci. 61 (11) (2016) 487–495.
[4] A. Barazandeh, et al., Predicting CpG islands and their relationship with genomic feature in cattle by hidden markov model algorithm, Iran. J. Appl. Anim. Sci. 6 (3) (2016) 571–579.
[5] A. Zarrabi, et al., Nanoliposomes and tocosomes as multifunctional nanocarriers for the encapsulation of nutraceutical and dietary molecules, Molecules 25 (3) (2020).
[6] N. Girard, et al., Thymic epithelial tumours: ESMO Clinical Practice Guidelines for diagnosis, treatment and follow-up, Ann. Oncol. 26 (Suppl 5) (2015) v40–v55.
[7] R. Álvarez-Velasco, et al., Clinical characteristics and outcomes of thymoma-associated myasthenia gravis, Eur. J. Neurol. 28 (6) (2021) 2083–2091.
[8] A.R. Punga, et al., Epidemiology, diagnostics, and biomarkers of autoimmune neuromuscular junction disorders, Lancet Neurol. 21 (2) (2022) 176–188.
[9] W. Jin, et al., Single-cell RNA-Seq reveals transcriptional heterogeneity and immune subtypes associated with disease activity in human myasthenia gravis, Cell Discov. 7 (1) (2021) 85.
[10] M. Mané-Damas, et al., Novel treatment strategies for acetylcholine receptor antibody-positive myasthenia gravis and related disorders, Autoimmun. Rev. 21 (7) (2022) 103104.
[11] R. Huda, Inflammation and autoimmune myasthenia gravis, Front. Immunol. 14 (2023) 1110499.
[12] M. Radovich, et al., The integrated genomic Landscape of thymic epithelial tumors, Cancer Cell 33 (2) (2018).
[13] R. Álvarez-Velasco, et al., Reduced number of thymoma CTLA4-positive cells is associated with a higher probability of developing myasthenia gravis, Neurology (R) Neuroimmunol. Neuroinflammation 10 (2) (2023).
[14] X. Liu, et al., Actin cytoskeleton vulnerability to disulfide stress mediates disulfidptosis, Nat. Cell Biol. 25 (3) (2023) 404–414.
[15] S.H. Masoudzadeh, et al., Dlk1 gene expression in different tissues of lamb, Iran. J. Appl. Anim. Sci. 10 (4) (2020) 669–677.
[16] F. Mohammadinejad, et al., Identification of key genes and biological pathways associated with skeletal muscle maturation and hypertrophy in Bos taurus, Ovis aries, and Sus scrofa, Animals 12 (24) (2022).
[17] L. Mohamadipoor Saadatabadi, et al., Signature selection analysis reveals candidate genes associated with production traits in Iranian sheep breeds, BMC Vet. Res. 17 (1) (2021) 369.
[18] M. Shahsavari, et al., Effect of fennel (Foeniculum vulgare) seed powder consumption on insulin-like growth factor 1 gene expression in the liver tissue of growing lambs, Gene Expr. 21 (2) (2022) 21–26.
[19] S.A.A.J. Ahmadabadi, et al., The effect of cannabis seed on DLK1 gene expression in heart tissue of Kermani lambs, Agric. Biotechnol. J. 15 (1) (2023) fa217–fa234.
[20] S.M.H. Safaei, et al., An origanum majorana leaf diet influences myogenin gene expression, performance, and carcass characteristics in lambs, Animals 13 (1) (2022).
[21] F. Bordbar, et al., Identification of candidate genes regulating carcass depth and hind leg circumference in simmental beef cattle using illumina bovine beadchip and next-generation sequencing analyses, Animals 12 (9) (2022).
[22] M. Mohammadabadi, et al., Fennel (Foeniculum vulgare) seed powder increases Delta-Like Non-Canonical Notch Ligand 1 gene expression in testis, liver, and humeral muscle tissues of growing lambs, Heliyon 7 (12) (2021) e08542.
[23] S. Shokri, et al., The expression of MYH7 gene in femur, humeral muscle and back muscle tissues of fattening lambs of the Kermani breed, Agric. Biotechnol. J 15 (2) (2023) 217–236.
[24] M. Mohammadabadi, et al., The effect of fennel (Foeniculum vulgare) on insulin-like growth factor 1 gene expression in the rumen tissue of Kermani sheep, Agric. Biotechnol. J. 15 (4) (2023) 239–256.
[25] S.M.H. Safaei, et al., Role of fennel (foeniculum vulgare) seed powder in increasing testosterone and IGF1 gene expression in the testis of lamb, Gene Expr. (000) (2023), 0-0.
[26] J.-Y. Liang, et al., A novel ferroptosis-related gene signature for overall survival prediction in patients with hepatocellular carcinoma, Int. J. Biol. Sci. 16 (13) (2020) 2430–2441.
[27] X. Li, et al., Identification and validation of stemness-related lncRNA prognostic signature for breast cancer, J. Transl. Med. 18 (1) (2020) 331.
[28] A. Mayakonda, et al., Maftools: efficient and comprehensive analysis of somatic variants in cancer, Genome Res. 28 (11) (2018) 1747–1756.
[29] N. Li, X. Zhan, Integrated genomic analysis of proteasome alterations across 11,057 patients with 33 cancer types: clinically relevant outcomes in framework of 3P medicine, EPMA J. 12 (4) (2021) 605–627.
[30] J. Tian, et al., CancerImmunityQTL: a database to systematically evaluate the impact of genetic variants on immune infiltration in human cancer, Nucleic Acids Res. 49 (D1) (2021) D1065–D1073.
[31] A. Marx, et al., The 2021 WHO classification of tumors of the thymus and mediastinum: what is new in thymic epithelial, germ cell, and mesenchymal tumors? J. Thorac. Oncol. 17 (2) (2022) 200–213.
[32] Y.-Q. Ao, et al., Recent thymic emigrants as the bridge between thymoma and autoimmune diseases, Biochimica Et Biophysica Acta. Reviews On Cancer 1877 (3) (2022) 188730.
[33] A. Iaiza, et al., Long non-coding RNAs in the cell fate determination of neoplastic thymic epithelial cells, Front. Immunol. 13 (2022) 867181.
[34] J. Zhuang, et al., Immune-related molecular profiling of thymoma with myasthenia gravis, Front. Genet. 12 (2021) 756493.
[35] M.L. Coleman, et al., Membrane blebbing during apoptosis results from caspase-mediated activation of ROCK I, Nat. Cell Biol. 3 (4) (2001) 339–345.
[36] L.M. Machesky, Deadly actin collapse by disulfidptosis, Nat. Cell Biol. 25 (3) (2023) 375–376.
[37] C. Masaoutis, et al., Unraveling the immune microenvironment of thymic epithelial tumors: implications for autoimmunity and treatment, Int. J. Mol. Sci. 23 (14) (2022).
[38] C.M. Lefeuvre, et al., Risk factors associated with myasthenia gravis in thymoma patients: the potential role of thymic germinal centers, J. Autoimmun. 106 (2020) 102337.
[39] C.A. Payet, et al., Central role of macrophages and nucleic acid release in myasthenia gravis thymus, Ann. Neurol. 93 (4) (2023) 643–654.
[40] H. Li, et al., Thymectomy and risk of generalization in patients with ocular myasthenia gravis: a multicenter retrospective cohort study, Neurotherapeutics 18 (4) (2021) 2449–2457.
[41] Y.-Q. Ao, et al., Immunotherapy of thymic epithelial tumors: molecular understandings and clinical perspectives, Mol. Cancer 22 (1) (2023) 70.
[42] A.C. Agrafiotis, et al., Tumor microenvironment in thymic epithelial tumors: a narrative review, Cancers 14 (24) (2022).
[43] M. Ballman, et al., Immunotherapy for management of thymic epithelial tumors: a double-edged sword, Cancers 14 (9) (2022).